

DESIGN AND PERFORMANCE OF WING CONFIGURATIONS FOR HIGH ALTITUDE SOLAR POWERED UNMANNED SYSTEM

Erdoğan MERMER¹, Abdülkadir KÖKER², D. Funda KURTULUŞ³, Erdal YILMAZ⁴,

^{1,2,4}TÜBİTAK UZAY

Ankara, TURKEY

³Middle East Technical University

Ankara, Turkey

ABSTRACT

In this paper, we performed some preliminary aerodynamic design and performance studies for a generic high altitude uninhabited and solar powered aerial vehicle. The paper focused on the performance of various wing geometries at different time periods of the year as well as at different altitudes up to 14 km. We considered six high lift airfoil sections such as Eppler 422 and S1223 at low Reynolds numbers from 8×10^5 to 1.5×10^6 to house solar panels on the wing upper surface. Our analysis showed that Eppler 422 airfoil section demonstrated better aerodynamic performance over the others. The power obtained from solar cell arrays mounted on the wing top surface area was calculated for different wing configurations including different airfoil sections, taper ratios, and sweep angles. The maximum power available from solar energy was compared for various wing configurations at different altitudes. It is concluded that going from sea level to 14 km, the required power to hold the airplane there jumps by about 250%.

INTRODUCTION

High Altitude and Long Endurance (HALE) Unmanned Aircraft Systems (UAS) are investigated widely in the world during the last couple of decades. The advantages of these systems are to create autonomous systems which have long flight endurance at high altitudes where almost no flight regulation are enforced and as well as an empty airspace with only a handful of air platforms operational (Nickol et al. 2007). Some of the high altitude systems are listed in Table 1. Other examples of these kind of aircrafts both manned and unmanned are Lockheed U-2A and U-2S, Strato-C, SR-71, AeroVironment Pathfinder, Helios, Darkstar.

Couple of projects within EU Framework exploited future use of high altitude unmanned systems. Among them CAPECON project [Okrent, 2005 Vol. 2] focused on medium and high altitude platforms, where one of them targeted solar energy for propulsion systems. UAVNET project [Okrent, 2005 Vol. 1] aimed to create an industrial basis for civilian use of unmanned systems. USICO project studied certification, safety, reliability in civilian use [Okrent, 2005 Vol.3].

The empty weight and maximum takeoff gross weight of some typical HALE UAS systems are presented in Figure 1.

¹B.Sc., TÜBİTAK Uzay, Email: erdinmermer@gmail.com

²B.Sc., TÜBİTAK Uzay, Email: kokabdul@hotmail.com

³Assoc. Prof. Dr. in Aerospace Engineering Department, METU, Email: dfunda@ae.metu.edu.tr

⁴Dr., TÜBİTAK Uzay, Email:erdal.yilmaz@tubitak.gov.tr

Table 1: *Examples of High Altitude Air Platforms*

Description	Perseus ¹	Condor ²	Global Hawk ³	Global Observer ⁴	Phantom Eye ⁵	Zephyr ⁶
Designer	USA NASA	USA Boeing	USA Northrop	USA AeroVironment	USA Boeing	UK QinetiQ
1 st Flight	1994	1998	1998	2005	2010	2010
Fuel	Petroleum	Petroleum	Petroleum	Liquid Hydrogen	Liquid	Solar
Length	8 m	15 m	14 m	25 m	16 m	6.1 m
Wing Span	22 m	59 m	35 m	79 m	65 m	10.5 m
TOGW	990 kg	9100 kg	4200 kg	4168 kg	4561 kg	53 kg
Flight Duration	24 hours	80 hours	36 hours	7 days	80 hours	14 days
Max. Ceiling	19 km	20 km	20 km	20 km	20 km	21 km
Payload	120 kg	825 kg	1000 kg	460 kg	206 kg	2.5 kg

¹[NASA 2009]

⁴[Aerovironment, 2010]

²[Boeing, 2012]

⁵[Boeing, 2012]

³[Northrop Grumman Corp, 2013]

⁶[Annabel, 2009]

Atmospheric conditions at high altitudes in terms of temperature, pressure, and density are very restrictive for air vehicle aerodynamics as well as for performance and propulsion system. Air temperature goes as low as minus 36.5 degrees even minus 60 degrees of celsius at night. All these effects reduces the speed of sound to 295 m/s hence making actual exposed Mach number about 10 percent higher compared to that of sea level. These conditions makes airfoil and wing design a challenging task.

Overall goal is to increase the endurance of these systems with the use of solar power as the propulsion system (solar regenerative (SR) power systems such as batteries and fuel cells) in order to obtain continuous flight through multiple day and night cycles. A low wing loading is necessary to reduce the power required to fly in the meantime to increase the solar-array area on the upper surface of the wing. These systems are used with photovoltaic arrays with Energy Storage System (ESS) to produce propulsive forces. The efficiency of solar cells, energy-storage roundtrip efficiency and energy-storage specific energy are the main important parameters for the propulsive system powered with solar energy.

Solar powered aircrafts requires very high wing span and high aspect ratio. However, increases in wing area causes dramatic increases in the weight of the aircraft. One way to solve this problem is flying wing configuration. In this configuration, due to absence of empennage and fuselage, total weight of the aircraft will be lower than conventional one. In solar powered UAV systems, power consumption is very significant due to fairly restricted solar panel area. Therefore they should fly at lower cruise speeds than other UAVs in order not to exceed available solar power. As a result, flying wing configuration gives large wing area, fairly low aircraft weight and low power requirement. In this study, flying wing configuration is investigated for three different wing geometries. Power requirements and solar power available values of these wings are analyzed and their performances are analyzed as a case study.

METHOD

Aerodynamics and Performance Analysis

The current paper focuses to analyze low Reynolds number airfoils and wing geometries for HALE UAV platform using publicly available XFLR5 program [Deperrois, 2012]. This program utilizes 3D panel method, lifting line theory, and vortex lattice methods in combinations. In our analysis, we assumed air condition at altitude of 14 km and higher. XFLR program is a 3-D panel method coupled with boundary layer. Air properties that correspond to three altitudes investigated are presented in Table 2.

Table 2: Air properties used in XFLR5 program

Altitude	Sea level	1 km	14 km
Air density [kg/m ³]	1.225	1.1117	0.22786
Kinematic viscosity [m ² /s]	0.000146	0.000158	0.000624
Reynolds number	1.5x10 ⁶	1.3x10 ⁶	0.814x10 ⁶

In order to choose the appropriate airfoil, some specifications have been taken into consideration. As operating conditions require low Reynolds number in the range of 8×10^5 to 1.5×10^6 , HALE UAV systems need to use airfoils with C_L and (L/D) ratios as high as possible. However, a solar powered aircraft should have the upper surface of the airfoils hence the wing as flat as possible with relatively low slopes in order to use sunray effectively that is maximizing direct exposure of Sun. Therefore, some airfoil analyses have been made and six airfoils were found to satisfy the conditions discussed above. In order to determine effective solar cell area, slopes of the upper surfaces have been calculated. The slopes whose absolute values are lower than a predetermined angle θ (as examples, $\theta=10^\circ$ and $\theta=25^\circ$ are chosen, see Figure 2) have been taken into consideration. Then, the projected area of the chord below certain value of the upper surface slope, named as solar cell area, has been determined. It is assumed that solar panels are not used on the wing area whose slopes are greater than θ degree. This slope threshold value is used due to the fact that at high sun light inclination angles of solar cells would not generate enough power even to lift its own weight. An algebraic equation can be derived this angle at a given time and position during the day, however for the sake of simplicity here we studied only 10 and 25 degrees of Sun beam inclination angles.

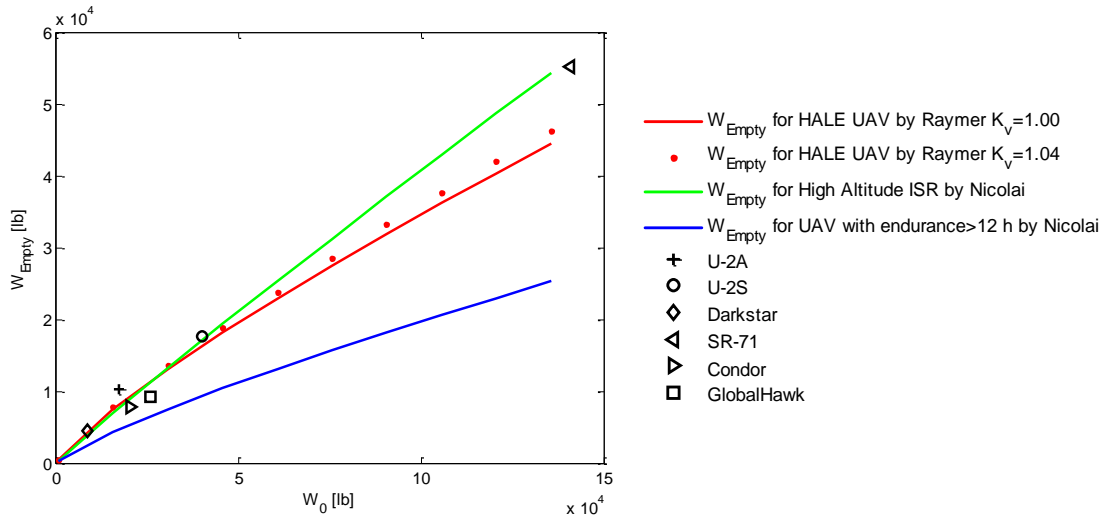


Figure 1: Empty Weight versus Maximum Takeoff Gross Weight of Different HALE UAS system

UAV Solar Power Calculation

An analytical approach is used in order to calculate solar irradiance per area for specified altitude. Formulations are given in Eq.1-Eq.5 [Duffie and Beckman, 1979]:

$$P_s = G_{sc} * A_s * v^2 * (\sin\delta * \sin\phi + \cos((h - 12) * 15) * \cos\delta * \cos\phi) \quad (\text{Eq. 1})$$

$$v^2 = \left(1 + 0.033 * \cos\left(\frac{360*d}{365}\right)\right) \quad (\text{Eq. 2})$$

$$\delta = 23.45 * \sin\left(\frac{360*(284+d)}{365}\right) \quad (\text{Eq. 3})$$

$$A_s = 0.5 * (e^{-0.65*\tau} + e^{-0.095*\tau}) \quad (\text{Eq. 4})$$

$$\tau = \frac{p}{p_0} * (\sqrt{1229 + (614 * \cos(\phi - \delta))^2} - 614 * \cos(\phi - \delta)) \quad (\text{Eq. 5})$$

In this equation, P_s (W/m^2) is the power used by the photovoltaic cells per unit area; $G_{sc} = 1347 \text{ W/m}^2$ is the solar constant; A is the alleviation coefficient of solar radiant flux through the atmosphere, d is the day of the year, ϕ is the aircraft latitude, h is the solar time, p is the static pressure at altitude considered and p_0 is the static pressure on the ground.

Power Required Calculation

The forces acting on the airplane are the lift L , and the drag D defined as:

$$\begin{aligned} L &= C_L * \frac{\rho}{2} * S * V^2 \\ D &= C_D * \frac{\rho}{2} * S * V^2 \end{aligned} \quad (\text{Eq. 6})$$

During level flight, Lift equals to weight and drag equals to thrust then, power required for level flight equals to drag times velocity:

$$P_{req} = D * V \quad (\text{Eq. 7})$$

Then using above equation, one can find power required for level flight:

$$P_{req} = \frac{C_D}{C_L^{3/2}} * \frac{g^3 * 2 * AR}{\rho} * \frac{m^{3/2}}{b} \quad (\text{Eq. 8})$$

Equation 8 is used for power required calculations where m is the mass, AR is the aspect ratio of the wing for three different wing configurations investigated in the study.

Solar Panel Properties

We investigated different solar panel types. In addition, future trends of the solar panel properties are taken into account. Different types of solar panels which is relevant for the current study are shown in Table 3 and the efficiencies corresponding to solar panels are used to calculate solar power available. Type 3 being one of the future trends of Gallium Arsenide type solar panels has efficiencies higher than 25% which can reach 30%. Even though Type 2 solar panel seems to have better properties than Type 1 solar panel cost of the Type 2 is too high. Type 1 is chosen for UAV solar power analysis. In this study, three different configurations are investigated and then, using type 1 and future trends' solar panels, solar power available for 3 different days of the year is calculated.

Table 3: Comparison of Solar Panel Properties [Alta Devices (2013), Sun Power Corp. (2013)]

Panel Properties	TYPE 1	TYPE 2	TYPE 3 (Future trend)
Dimension	125mm x 125mm	50 mm x 19.6 mm	66 mm x 31 mm
Efficiency	% 22	% 24	%25-30
Material	Mono crystalline silicon	GaAs	GaAs
Voltage reduction per °C	-1.8 mV / °C	-0.187% / °C	Not available
Power reduction per °C	-0.32% / °C	-0.08% / °C	Not available

RESULTS

For the desired qualifications, we found six different airfoil types to be appropriate in our solar cell area analyses. The first quantity is the need for high design lift coefficient (C_L) in order to carry the structural weight. The second one is the high L/D ratio in order to obtain high endurance according to the Breguet endurance approximation given in Eq. 7. The other important quantities are high solar cell area in order to maximize solar power used from the sunrays; low C_D values in order to operate the system by low thrust and low moment coefficient C_M in order to use relatively small empennage size.

$$E = \left(\frac{1}{c_t}\right) * \left(\frac{L}{D}\right) * \ln\left(\frac{W_0}{W_e}\right) \quad (\text{Eq. 9})$$

where c_t represents thrust specific fuel consumption W_0 aircraft gross weight and W_e aircraft empty weight.

Airfoil specifications in Table 2 have been found from XFLR5 results performed at different Reynolds numbers which corresponds to different operational altitude of HALE UAV considered. Figure 2 shows the shape of the airfoils selected and Figures 3-5 show C_l/C_d versus α ; C_l versus α and $C_l^{3/2}/C_d$ versus α graphs, respectively. Note that these factors are need in Eq. 6 and 7. In addition, upper surface areas whose tangencies are below θ angle (see Figure 2 for the angle definition) of 10° and 25° are calculated and these areas' horizontal projections are considered for total available cell area of the solar cell as a simple approximation and they are tabulated in Table 2. For more realistic calculations, instead of using the horizontal projections the curved upper surface area of the airfoils must be discretized into small segments and the corresponding solar irradiance should be integrated over the curved upper surface. The solar cell area calculations are given as the percentage of the projected areas to the chord line. The upper usable surface areas calculated in the tangency range in consideration in order to calculate maximum solar power obtained at solar noon condition. In these calculations, we found Eppler 422 airfoil to be the most appropriate for the current analysis due to its high design C_L value at maximum (L/D) ratio and low C_m values and highest solar power available for the conditions in consideration.

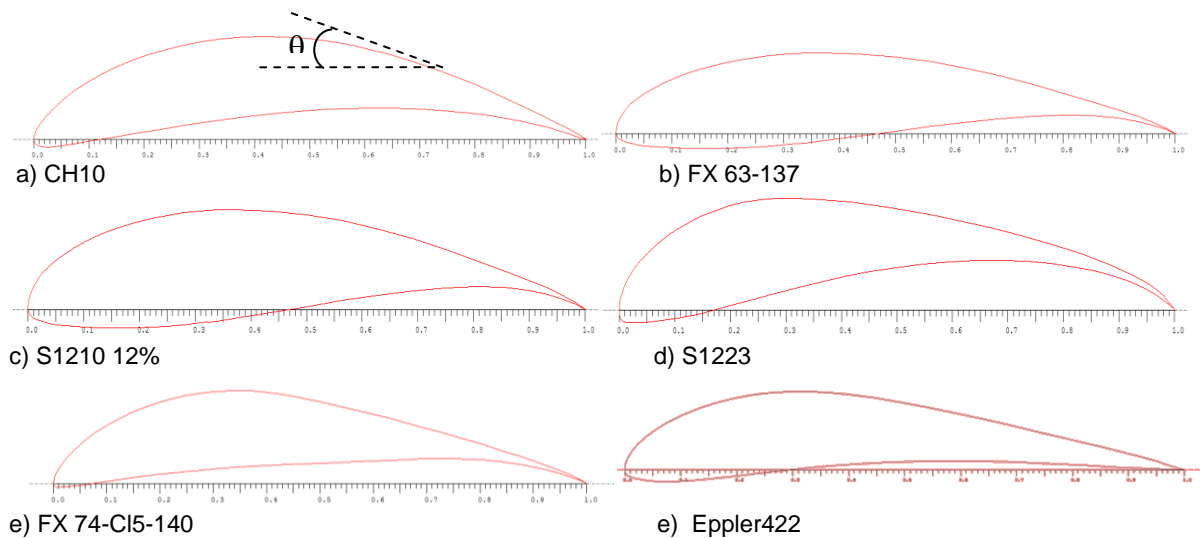


Figure 2: *Different Low Reynolds Number Airfoils Analysed*

Table 2: *Low Reynolds number airfoil parameters*

PROPERTIES	CH10	Fx63-137	S1210 12%	S1223	FX74cl5140	Eppler 422
$(t/c)_{max}$	12.8%	13.7%	12%	12.1%	13.1%	14%
Solar cell area $\theta=10^\circ$	58%	43%	48%	51%	18%	25.7%
Solar cell area $\theta=25^\circ$	78.41%	91.59%	85.46%	83.29%	82.70%	89.54%
<i>at sea level ($Re=1.5 \times 10^6$)</i>						
$(C_l/C_d)_{max}$	210	176	167	145	186	181
$C_l @ (C_l/C_d)_{max}$	1.77	1.17	1.57	1.91	2.15	1.58
$\alpha @ (C_l/C_d)_{max}$	5	2	4	7	8	9
$(C_l^{3/2}/C_d) @ (C_l/C_d)_{max}$	269	196	201	191	253	216
C_{lmax}	2.0418	2.05	2.07	2.35	2.23	1.935
α_{stall}	10	17	13	11	9	13
$C_d @ (C_{lmax})$	0.0201	0.068	0.045	0.0175	0.125	0.0155
$C_m @ (C_{lmax})$	-0.241	-0.142	-0.185	-0.193	-0.225	-0.095
$(C_l^{3/2}/C_d)_{max}$	269	200	201	191	253	216
$\alpha @ (C_l^{3/2}/C_d)_{max}$	5	4	4	7	8	9
<i>at 1 km altitude ($Re=1.3 \times 10^6$)</i>						
$(C_l/C_d)_{max}$	191	167	155	130	164	161
$C_l @ (C_l/C_d)_{max}$	1,75	1,27	1,66	1,98	1,92	1,66
$\alpha @ (C_l/C_d)_{max}$	5	3	5	7	12	9
$(C_l^{3/2}/C_d) @ (C_l/C_d)_{max}$	251	190	201	183	228	207
C_{lmax}	2,04	2,00	2,04	2,28	2,31	1,94
α_{stall}	10	17	13	13	12	14
$C_d @ (C_{lmax})$	0,021	0,095	0,05	0,035	0,031	0.0152
$C_m @ (C_{lmax})$	-0,24	-0,14	-0,175	-0,21	-0,215	-0,083
$(C_l^{3/2}/C_d)_{max}$	201	191	201	183	239	207
$\alpha @ (C_l^{3/2}/C_d)_{max}$	5	4	5	7	9	9
<i>at 14 km altitude ($Re=0.814 \times 10^6$)</i>						
$(C_l/C_d)_{max}$	166	151	130.78	113	133	133
$C_l @ (C_l/C_d)_{max}$	1.65	1.267	1.732	2,3	2.157	1.54
$\alpha @ (C_l/C_d)_{max}$	4	3	6	5	9	7
$(C_l^{3/2}/C_d) @ (C_l/C_d)_{max}$	216	179	185	151	189	160
C_{lmax}	2,05	1,91	2,05	2,3	2,3	1,92
α_{stall}	11	15	12	12	12	14
$C_d @ (C_{lmax})$	-0,27	0,06	0,043	0,03	0,025	0,023
$C_m @ (C_{lmax})$	-0,23	-0,14	-0,25	-0,23	-0,22	-0,08
$(C_l^{3/2}/C_d)_{max}$	216	179	185	154	197	175
$\alpha @ (C_l^{3/2}/C_d)_{max}$	4	4	6	8	10	10

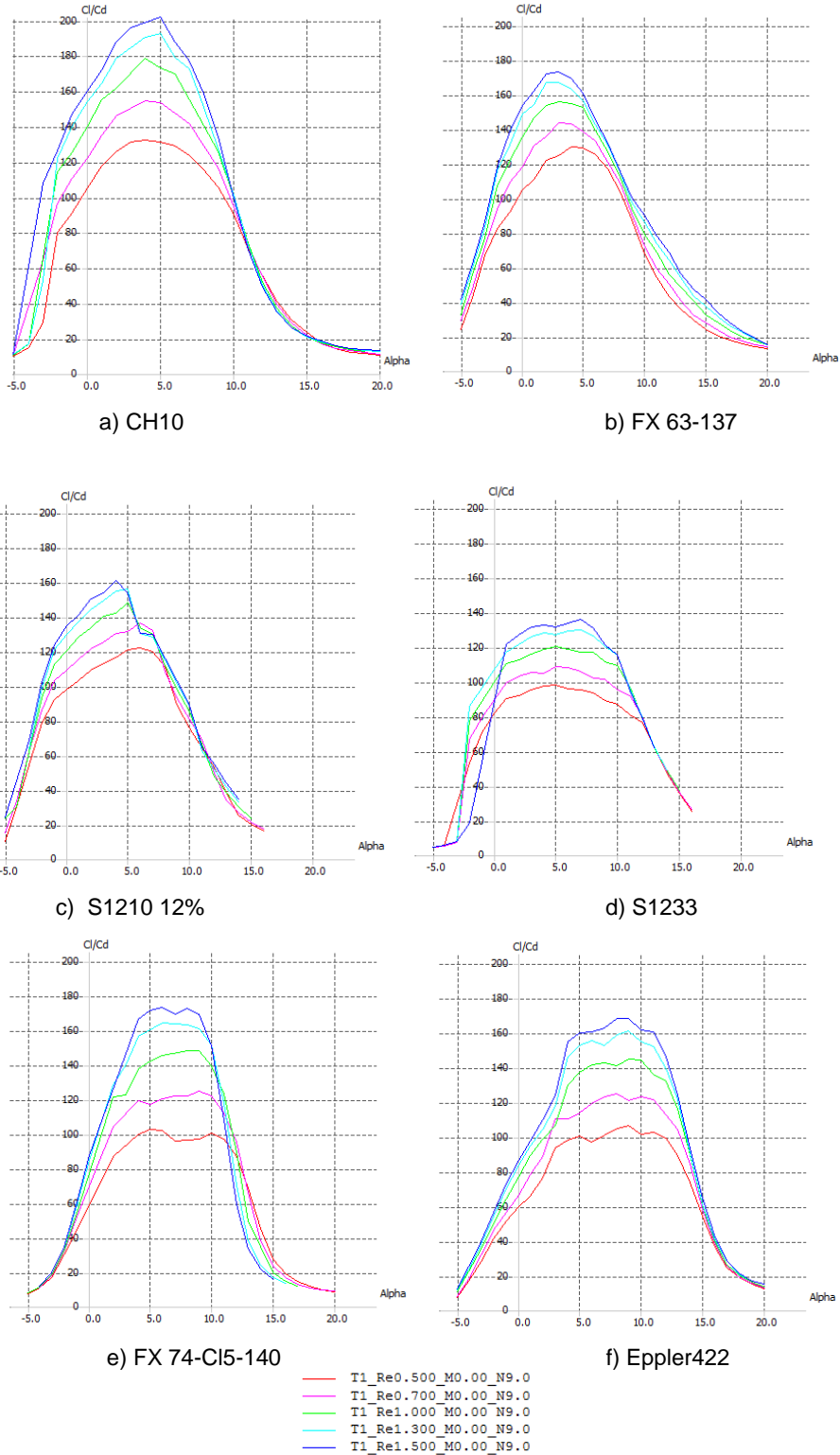


Figure 3: C_l/C_d versus angle of attack for different Airfoils

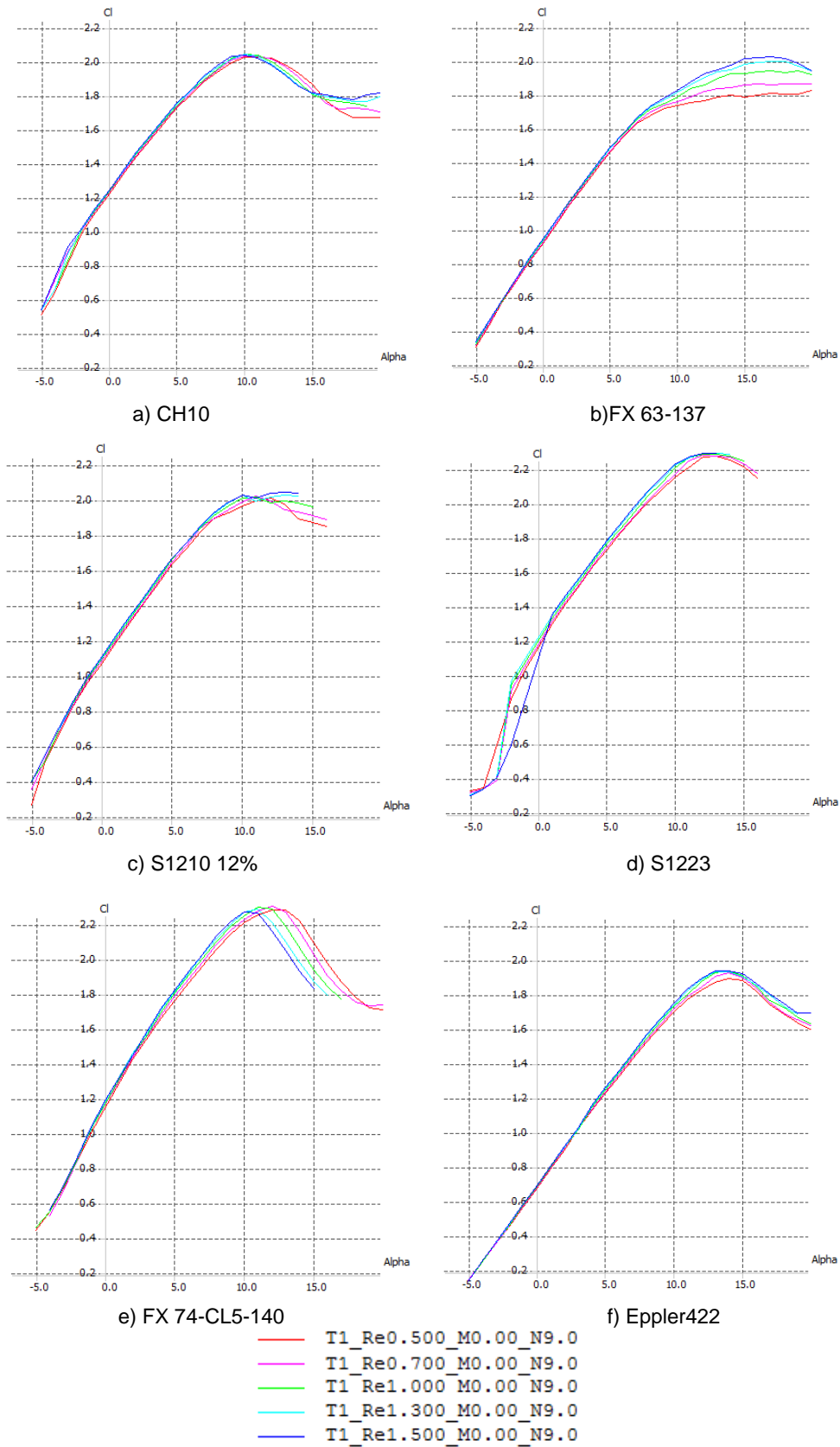


Figure 4: C_l versus angle of attack for different Airfoils

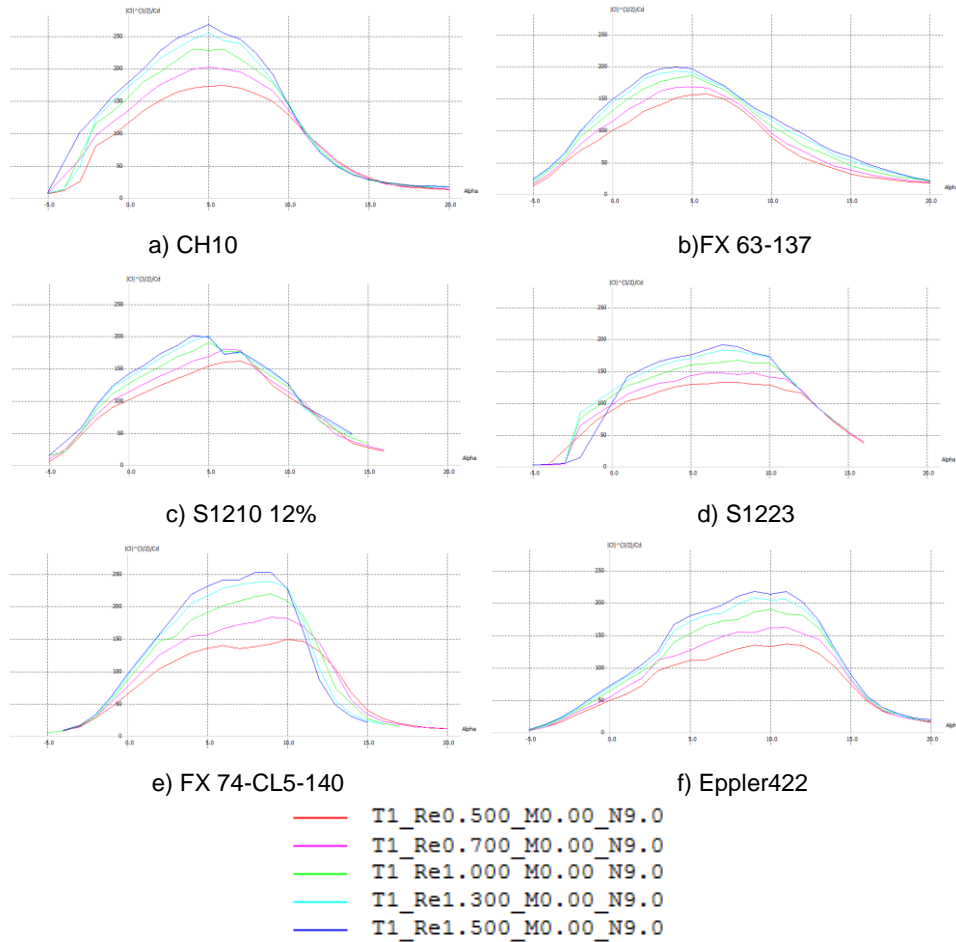


Figure 5: $(C_l^{3/2}/C_d)$ versus α for different Airfoils

Solar power calculation for different airfoils

Power distribution diagram is shown in Figure 6 for solar powered UAV systems. The figure shows different efficiencies taken into account during the calculation of the actual solar power value. Solar irradiance value for Ankara (approximately 1 km) and at HALE UAV operation altitudes of 14 km are shown in Figure 7b and Figure 7c, respectively. In addition, the results are also given at sea level condition (Figure 7a) for comparison purpose to check the power required value at this reference situation. The results given in Figure 6 and Figure 7 are found by using solar parameters and conditions given in Table 3.

Table 3: Solar Parameters

Solar Parameters	
\hat{G}_{sc}	1374 W/m ²
ϕ	39.927° (Latitude of Ankara)
d	80 (21 March) 172 (21 June) 355 (21 December)
p at 14 km	14170 N/m ²
p_0 at Sea Level	101325 N/m ²

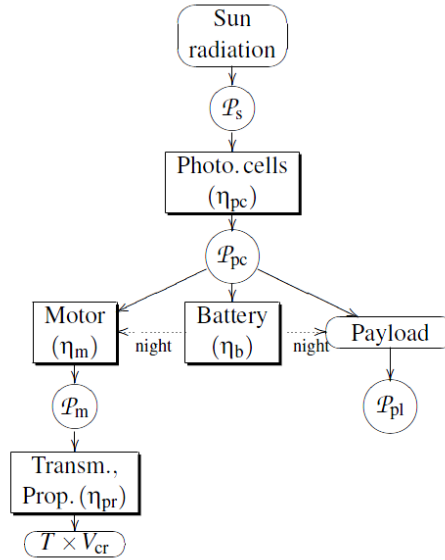


Figure 6: Power distribution of a typical solar powered UAV systems [Montagnier and Bovet, 2010]

Equation 8 shows total solar cell area, an equation in terms of solar cell area coefficients (C_{sa}) of airfoils for specific tangency angle of θ . The results are tabulated for airfoil upper surface's slope of $\theta < 25^\circ$. Wing area (S) is taken to be 80 m^2 for all cases investigated. Airfoil's solar cell area coefficients (C_{sa}) and total solar cell area, A , are presented in Table 5.

$$A = C_{sa} * S \quad (\text{Eq.10})$$

Table 4: Airfoil's solar cell area coefficients and total solar cell areas

PROPERTIES	CH10 (smoothed)	FX 63-137	S1210	S1223	FX 74_C15-140 (smoothed)	E422
Solar cell area coefficient, C_{sa} ($\theta < 25^\circ$)	78.40%	91.50%	81.40%	83.20%	82.70%	89.60%
A, Total solar cell area [m^2]	62.72	73.2	65.12	66.56	66.16	71.68

The actual power can be calculated as:

$$P = P_s * A \quad (\text{Eq. 11})$$

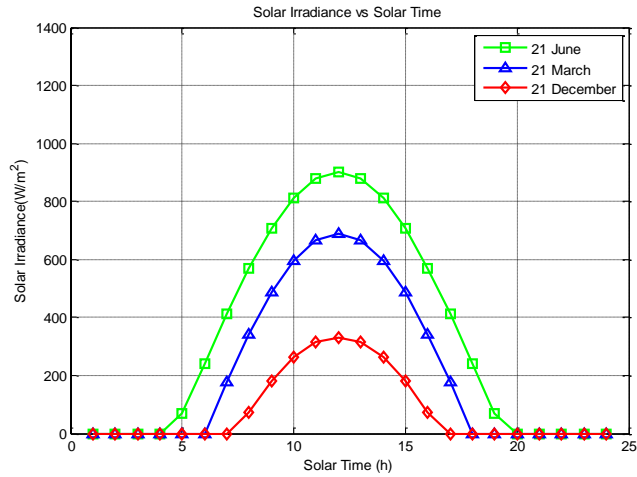
where P_s was the solar power irradiation given in Eq.1.

The total power for these different six airfoil configuration by considering the efficiencies [Ross, 2009] is given in Eq. 10. Figure 8 shows the total power versus solar time graph at 14 km and 1 km altitudes for 21 June (maximum solar energy storage day), 21 March and 21 December.

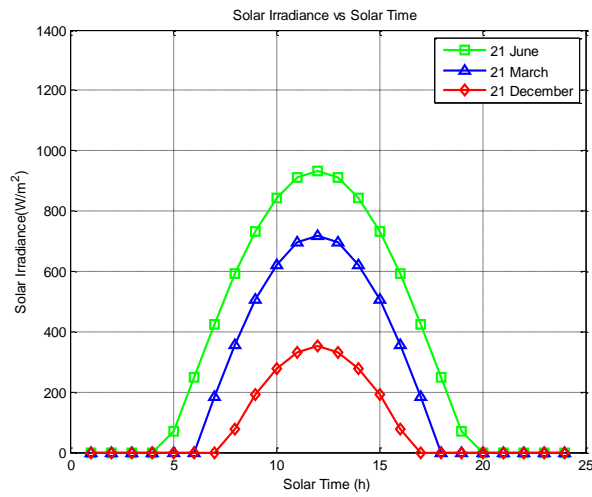
$$P = P_s * A * \eta_b * \eta_{sc} * \eta_m * \eta_p * \eta_c * \eta_{other} \quad (\text{Eq. 12})$$

where

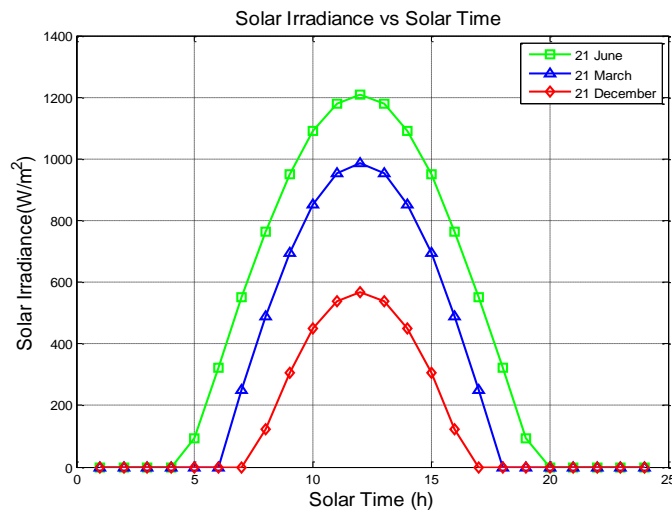
- $\eta_b = 96.5\%$ battery efficiency,
- $\eta_{sc} = 22\%$ solar cell efficiency,
- $\eta_m = 93\%$ electric motor efficiency,
- $\eta_p = 80\%$ propeller efficiency,
- $\eta_c = 98.5\%$ power converter efficiency
- $\eta_{other} = 94\%$ cable and other subsystem efficiencies.



a) at sea level



b) at 1 km altitude of Ankara latitude



c) at 14 km altitude of Ankara latitude

Figure 7: Solar Irradiance vs Solar Time graph for 3 days of the year (21 June, 21 March and 21 December)

Table 5: *Daily Total Available Energy for three different days of the year*

Daily Total Available Energy (kWh)	CH10	FX 74_CI5-140	S1223	S1210	FX 63-137	E422
@ Sea Level						
21 June	75.92	88.61	78.83	80.57	80.09	86.7
21 March	47.95	55.96	49.78	50.88	50.58	54.80
21 December	18.22	21.27	18.92	19.34	19.22	20.83
@ 1 km						
21 June	78.64	91.78	81.65	83.46	82.96	89.88
21 March	49.99	58.34	51.90	53.05	52.73	57.13
21 December	19.30	22.52	20.03	20.48	20.35	22.05
@ 14 km						
21 June	101.84	118.85	105.73	108.07	107.42	116.39
21 March	68.49	79.94	71.12	72.69	72.25	78.28
21 December	31.18	36.39	32.37	33.09	32.89	35.64

Table 6: *Daily Total Available Energy vs different solar panel efficiencies for Airfoil Eppler 422 at three different days of the year at 14 km altitude*

Daily Total Available Energy (kWh) using E422 Airfoil	Type 1 Solar Panel $\eta_{sc} = 22\%$	Type 3 Solar Panel $\eta_{sc} = 25\%$	Type 3 Solar Panel $\eta_{sc} = 30\%$
21 June	116.39	132.26	158.71
21 March	78.28	88.95	106.75
21 December	35.64	40.50	48.60

Various Wing Configuration Study

3 Different wing configurations are investigated in this study as shown in Figure 9. All 3 wings have the same reference wing area.

The wing with an AR of 20 to 26 with airfoil section of E244 is presented in Figure 9 and the 3D analysis obtained with XFLR5 program is compared with the corresponding 2D results in Figures 3-5. Although increased aspect ratio improves aerodynamic performance, span length can be considered as a restriction for the UAVs. Hangar capacities and departure runway are the main reason of the restrictions of the wing span. However, $C_L^{3/2}/C_D$ is an important parameter for HALE UAVs. The bigger the $C_L^{3/2}/C_D$ value the longer the endurance. Also high lift coefficient is another important demand due to low air density.

The main aim of the study is to compare different wing configurations at sea level, at 1 km (near Ankara) and 14 km. At higher altitudes desired aerodynamic properties such as $C_L^{3/2}/C_D$ and L/D decrease (Table 8).

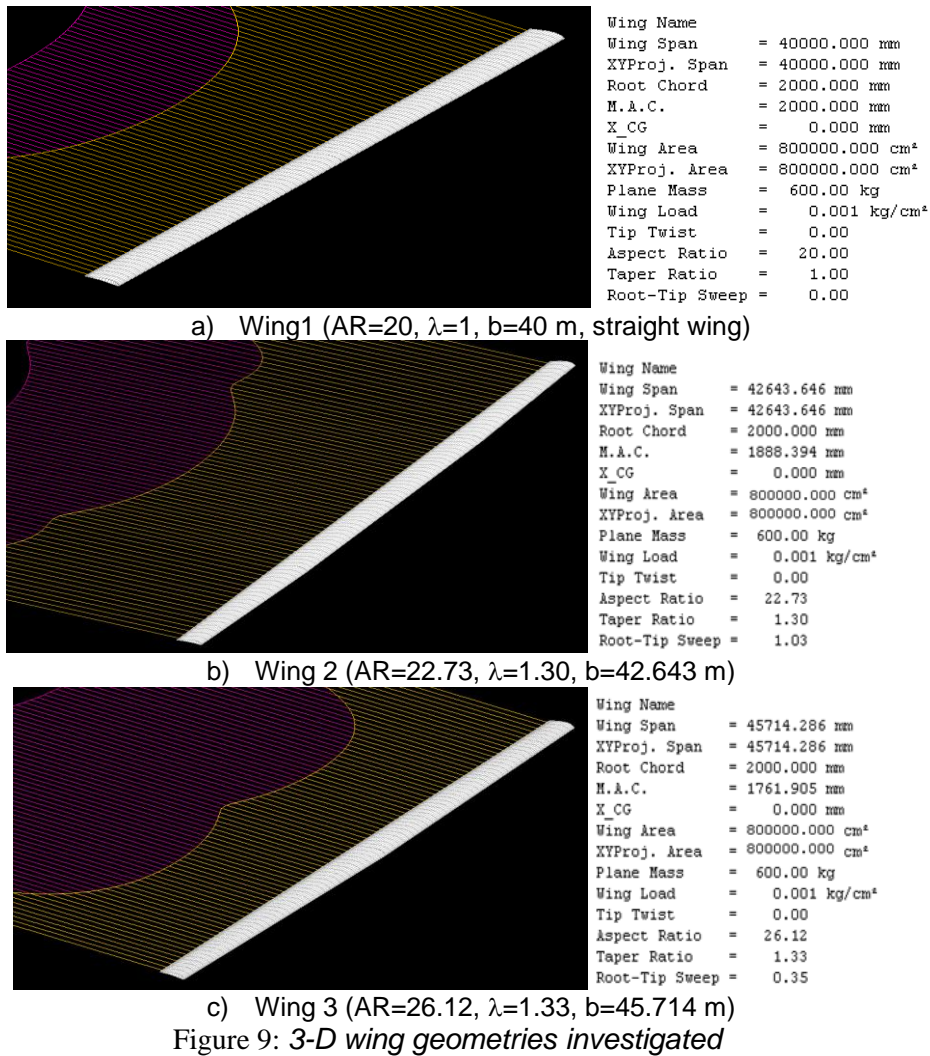


Figure 9: 3-D wing geometries investigated

Table 8: 3D Aerodynamics properties of three different wing geometries at different altitudes

Properties	Wing 1 Straight Wing AR=20.00 E422	Wing 2 Tapered Wing AR=22.73 E422	Wing3 Tapered Wing AR=26.12 E422
@ sea level			
$C_L @ 3^\circ$	0.94	0.9577	0.9776
$C_D @ 3^\circ$	0.024	0.0227	0.0214
$L/D @ 3^\circ$	39.14	42.2	45.61
$C_m @ 3^\circ$	-0.3624	-0.3693	-0.38
$C_m @ 0^\circ$	-0.29	-0.29	-0.38
$C_L @ 0^\circ$	0.64	0.65	0.66
$C_D @ 0^\circ$	0.0152	0.0146	0.014
$L/D @ 0^\circ$	41.9	44.48	47.25
$(L/D)_{max}$	41.9	44.48	47.35
$C_L @ (L/D)_{max}$	0.64	0.65	0.77
$\alpha @ (L/D)_{max}$	0	0	1
$C_L^{3/2} / C_D @ 0^\circ$	33.69	38.90	38.3
$C_L^{3/2} / C_D @ 3^\circ$	37.97	34.71	45.17
@ 1 km			
$C_L @ 3^\circ$	0.938	0.9577	0.9775
$C_D @ 3^\circ$	0.0241	0.0228	0.0217
$L/D @ 3^\circ$	39.0169	42.01	45.04
$C_m @ 3^\circ$	-0.3624	-0.3693	-0.38
$C_m @ 0^\circ$	-0.29	-0.29	-0.38
$C_L @ 0^\circ$	0.64	0.65	0.66

$C_D @0^\circ$	0.0152	0.0146	0.014
$L/D @0^\circ$	41.9	44.48	47.25
$(L/D)_{max}$	41.9	44.48	47.35
$C_L @ (L/D)_{max}$	0.64	0.65	0.77
$\alpha @ (L/D)_{max}$	0	0	1
$C_L^{3/2} / C_D @0^\circ$	33.67	38.4	37.9
$C_L^{3/2} / C_D @3^\circ$	37.92	32.7	44.8
@ 14 km			
$C_L @3^\circ$	0.94	0.9577	0.9771
$C_D @3^\circ$	0.0255	0.0227	0.0228
$L/D @3^\circ$	36.83	39,6	42.9
$C_m @3^\circ$	-0.3624	-0.4315	-0.4426
$C_m @0^\circ$	-0.29	-0.33	-0.34
$C_L @0^\circ$	0.64	0.65	0.66
$C_D @0^\circ$	0,0165	0.016	0.0155
$L/D @0^\circ$	38.69	40.62	42.65
$(L/D)_{max}$	38.7	40.9	43.3
$C_L @ (L/D)_{max}$	0.74	0.75	0.78
$\alpha @ (L/D)_{max}$	1	1	1
$C_L^{3/2} / C_D @0^\circ$	31.03	37.9	34.6
$C_L^{3/2} / C_D @3^\circ$	35.74	32.75	42.36

Power Required

Table 9 show initial parameters for the power required analysis. Three different wing geometries lift and drag coefficients are shown in Table 10. These cruise condition aerodynamic results are used to calculate the power required for the flying wing configurations.

Table 9: *Initial parameters for power required analysis*

Initial Parameters	
m	600 kg
b	40.00-42.64-45.71 m
AR	20.00-22.73-26.12

Table 10 *Wing C_L and C_D coefficients for three different altitudes and different wing geometries*

E422	$C_L @3^\circ$	$C_D @3^\circ$
@ 14 km		
Wing 1 Straight Wing AR=20.00	0.94	0.0255
Wing 2 Tapered Wing AR=22.73	0.9577	0.0227
Wing 3 Tapered Wing AR=26.12	0.9771	0.0228
@ 1 km		
Wing 1 Straight Wing AR=20.00	0.938	0.0241
Wing 2 Tapered Wing AR=22.73	0.9577	0.0228
Wing 3 Tapered Wing AR=26.12	0.9776	0.0217
@ sea level		
Wing 1 Straight Wing AR=20.00	0.94	0,024
Wing 2 Tapered Wing AR=22.73	0.9577	0.0227
Wing 3 Tapered Wing AR=26.12	0.9776	0.0214

Table 11 *Power required and daily energy required values for three different wing geometries*

E422 Airfoil Section is used	Power Required (kW)	Daily (24 hours) Energy Required (kWh)
@ 14 km		
Wing 1 Straight Wing AR=20.00	5.62	134.86
Wing 2 Tapered Wing AR=22.73	4.86	116.7
Wing 3 Tapered Wing AR=26.12	4.74	113.7
@ 1 km		
Wing 1 Straight Wing AR=20.00	2.41	57.84
Wing 2 Tapered Wing AR=22.73	2.21	53.04
Wing 3 Tapered Wing AR=26.12	2.01	48.24
@ sea level		
Wing 1 Straight Wing AR=20.00	2.28	54.72
Wing 2 Tapered Wing AR=22.73	2.09	50.16
Wing 3 Tapered Wing AR=26.12	1.92	46.08

It is clearly seen that tapered wing and higher aspect ratio reduce the power requirement for the air vehicle. From sea level to 14 km power required increased by almost 250%. Wing 3 Tapered Wing AR=26.12 configuration is chosen for the current UAV design due to its lowest power requirement. In the solar power calculation section, it is checked whether solar cell power can meet above daily power requirements. As seen on Table 11, for case wing 1, wing 2, wing 3 @ 14 km, energy required is respectively 113.7, 116.7 and 134.86 kWh. Solar power can also satisfy these requirements on certain time period in a year depending on the solar panel efficiency. Flight time period of the solar powered UAV system at condition of $E_{available} > E_{required}$ is calculated for three different solar panel efficiencies in Table 12.

Table 12 *Flight time period for $E_{available} > E_{required}$ condition for three different solar panel efficiencies at 14 km altitude*

Flight Time period for $E_{available} > E_{required}$ for 14 km altitude	Solar panel with efficiency of 22%	Solar panel with efficiency of 25%	Solar panel with efficiency of 30%
Wing 1 ($E_{required}=134.9\text{kWh}$)	Requirement not satisfied	Requirement not satisfied	21 April – 21 August
Wing 2 ($E_{required}=116.7\text{kWh}$)	Requirement not satisfied	2 May – 9 August	7 April – 10 September
Wing 3 ($E_{required}=113.7\text{kWh}$)	1 June - 10 July	25 April – 15 August	30 March – 12 September

From Table 12, it is seen that Wing 1 and Wing 2 configurations can never fly with solar panel efficiency of 22% and Wing 1 also cannot fly with a solar panel having efficiency of 25%. Also flight periods of Wing 1 and Wing 2 are fairly low compared to Wing 3 for future trend solar power efficiencies of 30%. Wing 3 is the best configuration for solar powered UAV among other cases investigated. It is also seen that in order to expand the flight time, solar panel efficiency should be increased. Solar panel efficiency increase from 22% to 25% causes approximately 70 day increase of flight time period and an increase from 22% to 30 % causes 92 day increase in flight time period for wing 3 configuration. It should be noted that increasing trend of panel efficiencies will not result a linear increase of flight time period since solar irradiance starts to be lower in autumn and winter months. It should be noted that, a detailed analysis of solar beam angular effect will be performed as future work to calculate exact power available over the airfoil surfaces rather than the approximate calculations used in the current study.

References

- Aerovironment (2010) Global Observer. .retrieved from: <http://www.avinc.com/globalobserver/>
- Alta Devices (2013) Retrieved from: http://www.altadevices.com/pdfs/single_cell.pdf
- Altman A. Ph.D. thesis (2000) : A Conceptual Design Methodology for Low Speed High Altitude Long Endurance Unmanned Aerial Vehicles
- Annabel R. (2009) “Zephyr: A High Altitude Long Endurance Unmanned Air Vehicle” Master Thesis ,Department of Physics University of Surrey,
- Boeing Corp. (2012) Phantom Eye Retrieved from: http://www.boeing.com/farnborough2012/pdf/Bkgd_PhantomEye_0612.pdf
- Boeing Corp. (2012) Condor Retrieved from: <http://www.boeing.com/history/boeing/condor.html>
- Duffie J. A., Beckman W. A. (2013) Solar energy thermal processes, 4th edition, John Wiley and Sons, Inc.
- Gundlach J. (2012) Designing Unmanned Aircraft Systems, AIAA Education Series
- Montagnier, O., Bovet, L. (2010) Optimisation of a solar-powered high altitude long ednurance uav, in: 27nd International Congress of The Aeronautical Sciences (ICAS), Nice, France.
- NASA, (2009) Perseus Retrieved from: <http://www.nasa.gov/centers/dryden/history/pastprojects/Erast/perseusb.html>
- Nickol C. L., Guynn M. D., Kohout L.L., Ozoroski T. A. (2007) *High Altitude Long Endurance UAV Analysis of Alternatives and Techology Requirements Development*, NASA TP-2007-214861
- Nicolai L. M., Carichner G. E. (2010) *Fundamentals of Aircraft and Airship Design Volume I — Aircraft Design*, AIAA Series
- Northrop Grumman Corp. (2013) Global Hawk. Retrieved from: <http://www.northropgrumman.com/Capabilities/GlobalHawk/Pages/default.aspx>
- Okrent. M. (2005)“25 Nations For An Aerospace Breakthrough European Civil Unmanned Air Vehicle Roadmap.” Volume 2 – Action Plan. Submitted On Behalf Of The European Civil UAV FP5 R&D Program Members.
- Okrent M. (2005) “25 Nations For An Aerospace Breakthrough European Civil Unmanned Air Vehicle Roadmap.” Volume 1 – Overview. Submitted On Behalf Of The European Civil UAV FP5 R&D Program Members.
- Okrent. M. (2005) “25 Nations For An Aerospace Breakthrough European Civil Unmanned Air Vehicle Roadmap.” Volume 3 – Strategic Research Agenda. Submitted On Behalf of The European Civil UAV FP5 R&D Program Members.
- Raymer D. P.,(2006), *Aircraft Design: A Conceptual Approach*, 4th edition, AIAA Education Series
- “Global Stratospheric Change—Requirements for a Very High Altitude Aircraft for Atmospheric

Research,” workshopreportTruckee, CA, 15–16 July 1989, NASA Conf. Publ. No. CP-10041, 1989.

Sun Power Corp. (2013) Retrieved from: <http://us.sunpowercorp.com/homes/products-services/solar-panels/x-series/>

Deperrois A. (2012) XFLR5 Program, Retrieved from: <http://www.xflr5.com/xflr5.htm>